Nonlinear Effects of Intraspecific Competition Alter Landscape-Wide Upscaling of Ecosystem Function

Chelsea J. Little[1,2], Emanuel A. Fronhofer[1,2,3], Florian Altermatt[1,2]

[1]Department of Evolutionary Biology and Environmental Studies, University of Zurich, Winterthurerstrasse 190, CH-8057 Zürich, Switzerland.

[2]Eawag, Swiss Federal Institute of Aquatic Science and Technology, Department of Aquatic Ecology, Überlandstrasse 133, CH-8600 Dübendorf, Switzerland.

[3]ISEM, Univ Montpellier, CNRS, EPHE, IRD, Montpellier, France.

Corresponding author: Chelsea J. Little (chelseajean.little@eawag.ch)

Keywords

Decomposition, Jensen's inequality, leaf litter, macroinvertebrates, scaling up, shredders

Abstract

A major focus of ecology is to understand and predict ecosystem function across scales. Many ecosystem functions are only measured at local scales, while their effects occur at a landscape level. Here, we investigate how landscape-scale predictions of ecosystem function depend on intraspecific competition, a fine-scale process. Specifically, we experimentally investigated the effect of intraspecific density of shredding macroinvertebrates on associated leaf litter decomposition, a key function in freshwater ecosystems. Across two species, we found that leaf processing rates declined with increasing density following a power law, likely due to interference competition. To demonstrate consequences of this nonlinearity, we upscaled estimates of leaf litter processing from shredder abundance surveys in 10 replicated headwater streams. In accordance with Jensen's inequality, applying density-dependent consumption rates reduced estimates of catchment-scale leaf consumption up to 60-fold versus using density-independent rates. Our work highlights the need for spatially-explicit upscaling which accounts for intraspecific interactions.

Introduction

In an era of ongoing global change, a growing focus of ecology is to understand what controls ecosystem functioning, and to predict future scenarios of ecosystem function and services. Biodiversity is an important determinant of ecosystem functioning because of the traits, functions, and dynamics of individual species (Tilman et al. 2014; Eisenhauer et al. 2016; Grace et al. 2016). The number of species in an ecosystem determines its functioning not just by summing these traits and functions, but also through the interaction between organisms, which can be synergistic or antagonistic (Gessner et al. 2010; Carrara et al. 2015). Thus, the relative abundance of species is important because the presence of a strongly-dominant species, for example, can influence the relationship between biodiversity and ecosystem function (Dangles and Malmqvist 2004; Isbell et al. 2013).

However, despite the clear effect of dominant species on ecosystem function, the density of organisms is rarely explicitly considered when estimating ecosystem function. This is surprising, because intraspecific, density-dependent interactions are recognized as important in almost all disciplines of ecology. For example, they are a key requirement for the maintenance of biodiversity according to modern coexistence theory (Chesson 2000; McPeek 2012), and many aspects of population dynamics are controlled by density (Hassell et al. 1976; Brook and Bradshaw 2006). Logically, then, the functions performed by organisms are also under density-dependent control, in which case ecosystems with differing abundances of a particular species could have different dynamics, function, and fates. It is also a surprising gap because variation in intraspecific density is ubiquitous in nature: there is considerable variation in species abundances through space and time (Hanski 1990).

Thus, density-dependent control of ecosystem function is not just potentially substantial in magnitude, but could be widespread. Yet, the consequences of this mechanism for landscape-level ecosystem function remain unexplored. Understanding the shape of a density-ecosystem function (henceforth DEF) relationship is crucial, as non-linear relationships abound and affect the accuracy of upscaling (Harvey 2000). Analogous to functional- and temperature-response curves, non-linear DEF relationships would mean that upscaling based on knowledge of ecosystem function at one scale could greatly over- or under-predict gross rates at a broader scale (Ruel and Ayres 1999; Kingsolver 2009; Denny and Benedetti-Cecchi 2012).

Decomposition in freshwater ecosystems may be a particularly relevant context for DEF relationships. Decomposition regulates resource cycling, and is particularly important in aquatic systems where terrestrial detritus can make up a large portion of resource fluxes (Gounand et al. 2018). Communities of species contributing to decomposition are characteristically less complex than in freshwater than terrestrial ecosystems (Hieber and Gessner 2002), and as a result density variation in those few species could have a large impact (Jonsson and Malmqvist 2003; Klemmer et al. 2012). Yet decomposition is less frequently considered in ecosystem function frameworks than terrestrial biomass production (Cardinale et al. 2011), where a greater diversity of species contribute to ecosystem function through time. This may be one reason why DEF relationships have rarely been explored: biomass is often considered an ecosystem function rather than an explanatory mechanism.

Here, we investigate the relationship between intraspecific density of two aquatic macroinvertebrate shredders and their rate of leaf litter processing. We then use these DEF relationships to upscale leaf litter processing estimates to catchment levels based on spatial variance in intraspecific density observed across multiple

independent headwater stream networks. Previous upscaled estimates of the effect of shredder species turnover on ecosystem function assumed density-independence of leaf processing rates and furthermore assumed equal densities throughout a catchment (e.g., Piscart et al. 2011). By contrast, we incorporate spatial variance in abundances for two reasons. First, a previous meta-analysis of laboratory studies indicated density-dependence in per-capita leaf consumption rates (Little and Altermatt 2018*a*). Secondly, in this group of shredding macroinvertebrates typically one species dominates locally, but the dominant species varies in abundance over orders of magnitude within a catchment (Welton 1979; Van den Brink et al. 1991; Altermatt et al. 2016; Little and Altermatt 2018*b*). This creates an ideal scenario to test the concept of a DEF relationship whereby the abundance of these key taxa, rather than species richness, could control decomposition and thus would need to be considered in upscaling predictions.

Methods

Study Organisms

We experimentally assessed effects of intraspecific density on leaf shredding rates by two freshwater amphipod (Crustacea, Amphipoda) species: *Gammarus fossarum* (Koch), a relatively small species native to Central Europe, and *Dikerogammarus villosus* (Sowinsky), a relatively large species native to the Ponto-Caspian region which has recently invaded many regions worldwide (Van den Brink et al. 1991; MacNeil et al. 2012). Collection and maintenance of study organisms are described in the Supplementary Material.

Mesocosm Experiments

Mesocosms were built from 2 L plastic containers with 0.4 m^2 of bottom surface area, placed in a flowing-water rack system with a mixture of stream and tap water. Conditioned naturally senescent alder leaves totalling 1.5 g (dry weight) were placed in each mesocosm. For each species, mesocosms were set up with fixed densities of the target amphipod species: 50 replicates with one individual, 20 replicates with two individuals, 10 with five individuals, 10 with 10 individuals, six with 20 individuals, and six with 30 individuals per mesocosm. This 30-fold density range is smaller than the >100-fold density range commonly observed in stream reaches (Little and Altermatt 2018*b*). The unbalanced number of replicates for each density was chosen because per-mesocosm leaf consumption was expected to be more variable in replicates with fewer amphipods.

The leaf consumption experiments were run for 19 (*G. fossarum*) and 12 (*D. villosus*) days, respectively, at which point leaves from the mesocosms were collected and dried for 48 h at 60 ˚C, then weighed to calculate mass loss from the beginning of the experiment. Amphipods were counted every two to three days throughout the experiments to track mortality; overall, survival was 89.3% for *G. fossarum* and 95.1% for *D. villosus*. These mortality estimates were used to calculate an average amphipod density (individuals per square meter) that the mesocosm experienced over the length of the experiment. At the end of the experiment, amphipods were sacrificed, dried for 48 h at 60 ˚C, and weighed. Individuals which died during the course of the experiment were assigned the global average weight of all amphipods across the experiment. The average daily biomass in a mesocosm (mg m^{-2}) was then calculated as the average density multiplied by the average weight of all individuals in the mesocosm. Two outliers were removed from the *G. fossarum* dataset and three from the *D. villosus* dataset, because their consumption rate estimates were over three

standard deviations from the mean and also substantially higher than any we had measured in previous experiments (Little and Altermatt 2018*a*), and we did not feel we could rule out measurement error as an explanation.

DEF models

For both amphipod species, we tested for the effects of density on leaf consumption using nonlinear models in R version 3.5.0 (R Core Team, Vienna, Austria). Initial data exploration and linear models using transformed and non-transformed data showed that these relationships were linear in log-log space (see Supplementary Material for details, and Figure S1). Therefore we created negative exponential models using the gNLS function in the 'nlme' package version 3.1-137 (Pinheiro et al. 2013) and weighted data points by the variance in the response variable, since there was higher variance around high estimates of leaf litter consumption across the experiment. For each species we created separate models of the relationships between amphipod density and per-amphipod daily leaf consumption, and between amphipod biomass and biomass-adjusted daily leaf consumption.

Upscaling to Real Catchments

We upscaled estimates of leaf litter processing to the catchment level by pairing the derived DEF equations with spatially resolved population density data from field surveys. We had previously assessed amphipod abundance in ten headwater stream catchments in eastern Switzerland predominantly inhabited by *G. fossarum*, where *D. villosus* was present only rarely at the outlets (Altermatt et al. 2016; Little and Altermatt 2018*b*); the species is more common in rivers (Van den

Brink et al. 1991). The goal of upscaling was to demonstrate the consequences of nonlinear DEF relationships, so since shape of the relationship was similar in the two species, we performed the analysis based only on the *G. fossarum* DEF function. The full details of the field surveys are described in Little and Altermatt (2018*b*), but briefly, sampling points were established in April 2015 in every ~250 m section of each stream. Amphipods were collected using a kicknet and their density was estimated on a logarithmic scale (0, 1–10, 11–100, 101–1000, or >1000 individuals per 1 meter-long stream segment). Below, we refer to these abundance estimates as 'bins'.

For upscaling, we longitudinally divided each stream's mapped watercourse (Swisstopo 2007) into one-meter segments and used two different methods to estimate the total abundance of amphipods in the catchment: inverse distance weighted interpolation and proportional estimation. We simulated spatial abundances of amphipods 1000 times per catchment using each method, and averaged over the simulations to extract catchment-wide predictions of abundance and processing (see below).

Inverse distance weighting (IDW) produces interpolated data that varies smoothly in space as a function of distance from measured sampling points, based on the assumption that points close to each other are more similar. Each IDW simulation began by assigning the catchment's sampling points (n = 9–15, depending on the catchment) to a random abundance value within their observed abundance bin (e.g., a random number between 11 to 100 for a bin with 11–100 individuals). Then using the package 'gstat' (Pebesma 2004), each one-meter segment was assigned an abundance based on its distance from these 9–15 assigned points.

With the proportional estimation method, we removed the assumption that nearby reaches are more similar to each other and instead focused only on capturing the observed variation in surveyed abundances. With this method, we recorded the proportion of a catchment's sampling points which belonged to each abundance bin (i.e. proportion of sampling points with zero amphipods, proportion with 1–10 amphipods, etc.) and created a probability distribution of abundance bin assignment for the catchment. For a simulation, every one-meter stream segment was randomly assigned to an abundance bin based on this probability function, and then the segments were assigned random abundances from within the range of their assigned bins (e.g., assigned to the 1–10 amphipod bin, and then assigned a random number between 1 and 10).

For each simulation, the one-meter segments were summed to produce a catchment-level abundance estimate. The 1000 simulations per catchment (per method) were summarized with means and 95% confidence intervals.

We estimated whole catchments' total leaf litter processing rate per day based on these abundance estimates, under two scenarios. In Scenario 1, we multiplied the global average processing rate from the *G. fossarum* density experiment (i.e., average across all densities) by the total population size of the catchment, a common way to upscale consumption estimates (for example, Piscart et al. 2011). In Scenario 2, we used the spatially-varying amphipod densities derived from the two estimation methods, and applied the experimentally-derived *G. fossarum* DEF function from to each one-meter stream segment before summing to the catchment level.

Results

Our experimental data fit negative power laws relating per-capita consumption rates to density (for fitting details, see Supplementary Material). This was true both when relating individual density to per-capita leaf consumption (Figure 1), and density of biomass to biomass-adjusted leaf consumption (Figure S4). To confirm that these derived relationships explained the density-dependent relationship with per-capita consumption rates, we calculated predicted per-mesocosm total leaf consumption along a continuous gradient of amphipod densities. These curves (solid lines in right panels of Figure 1) reasonably matched the actual per-mesocosm leaf consumption rates, while linear extrapolations based on density-independent, constant per-capita consumption rates overestimated total leaf consumption by orders of magnitude for any density greater than a few amphipods per square meter (Figure 1).

Next, we performed upscaling to estimate amphipod abundance in the ten study catchments. Estimates of whole-catchment abundance ranged from hundreds (808 in Dorfbach) to millions (1.46 million in Mannenbach) of amphipods using the inverse distance weighted estimation method (Table 1), and from thousands (1,590 in Dorfbach) to millions (1.43 million in Seebach) using proportional estimation (Table S2).

In an example catchment, the Chesselbach (for all other catchments, Table 1, Table S2, and Figures S5–S13), inverse distance weighted interpolation from 13 sampling points (Figure 2) produced an estimate of ~720,000 amphipods in the catchment (mean of 1000 simulations: 720,719; 95% CI 709,980–731,456). Using the mean experimental per-capita consumption rate (12 mg amphipod^{-1} day^{-1}) to derive leaf processing (Scenario 1) yielded a mean of 8.8 kg of leaf litter processed per day. Applying the experimentally-derived negative exponential DEF relationship to the spatially-varying interpolated densities in the catchment (Scenario 2) resulted in a

markedly lower predicted processing rate, in this case a mean of 0.3 kg per day. Indeed, in all but one (the most sparsely occupied) catchment, estimates of total leaf litter processing were lower using the experimentally-derived DEF relationship than when using a density-independent processing rate (Table 1). The mismatch was substantial: not accounting for density dependence resulted in leaf processing rates up to 60 times higher in some catchments. Results were similar when based on proportional abundance estimations (Table S2).

Discussion

As ecology moves towards a more predictive science, a central challenge is that the underlying mechanisms leading to an observed response – for example, ecosystem function – are occurring at a different scale (Levin 1992). In this context, the nonlinear relationships abundant in nature present challenges for upscaling. Often, it may be necessary to incorporate variance in the explanatory variable, not simply mean values, for predictions to be accurate (Ruel and Ayres 1999; Melbourne and Chesson 2005; Denny and Benedetti-Cecchi 2012). Using experimental manipulations at the level of individual small organisms, we found that local population density had a strong effect on leaf litter processing rates of two dominant freshwater detritivores, and thus their per-capita contribution to ecosystem function. At the reach scale, the shape of this density-ecosystem function (DEF) relationship meant that estimated ecosystem function was similar across stream reaches, even when there was substantial spatial heterogeneity in organismal abundances. At the landscape scale, that is, the scale of riverine networks (Altermatt 2013), the shape of this nonlinear relationship had strong implications for upscaled predictions of ecosystem function, because population density increases much faster than its corresponding ecosystem

function. As a result, ecosystem function predictions based on our experimentally-derived DEF relationship were more than an order of magnitude lower than predictions made using more simplistic, mean-based estimates. Thus, neglecting the role of density may systematically bias estimates of ecosystem function.

Intraspecific competition for resources is an essential regulator of population dynamics. Here, we demonstrate that intraspecific density could also regulate leaf litter processing, a key ecosystem function globally providing terrestrial resources to freshwater ecosystems (Gounand et al. 2018). Previously, leaf litter processing was shown to vary nonlinearly with abundance of macroinvertebrates, which was attributed to intraspecific resource competition at high densities (Klemmer et al. 2012). However, in our experiments, resources were not limiting, and per-capita leaf processing decreased even at relatively low densities. Thus, we find it more likely that interference competition (Schoener 1983) generated these nonlinearities. In the broader context of upscaling, however, both types of competition are important as they could shape DEF relationships.

One main consequence of a nonlinear DEF relationship is that predictions at the landscape scale become challenging. This is especially relevant for organisms that are known to vary in their abundance locally over several orders of magnitude, such as the dominant shredders studied here. In our case, neglecting the role of density would lead to vast overestimates of ecosystem function; in other contexts (species, relationships, and functions) the reverse may be true. Connecting nonlinear population dynamics and spatial heterogeneity led to the development of scale transition theory (Melbourne and Chesson 2005; Chesson 2012), which has been applied to populations and communities and should be expanded to ecosystem-level processes.

Our results expand the current understanding of biodiversity effects on ecosystem function (BEF) to include density-dependent effects on ecosystem function (DEF), recognizing that non-linear dependencies are prevalent and important (Grace et al. 2007; Tilman et al. 2014). In fact, the two frameworks are related: release from intraspecific competition has been discussed as a mechanism through which increasing species richness accelerates ecosystem function (Jonsson and Malmqvist 2003; Weis et al. 2007; Patrick 2013). Connecting plot- and patch-level results to real, complex ecosystems and larger scales is recognized as one of the biggest challenges in ecosystem function research, with some debate as to the success of efforts to date (Hewitt et al. 2007; Snelgrove et al. 2014; Eisenhauer et al. 2016; Wardle 2016). Our results suggest that in some contexts, DEF may be more important than BEF, but that this does not diminish the need for upscaling to be spatially explicit or to account for organisms' interactions.

Acknowledgements

The authors thank two students, Georg Flückiger and Sascha Brunner, for help with the *G. fossarum* experiment, and thank Samuel Hürlemann and Remo Wüthrich for help in the lab and field. CJL would like to thank the Eawag Eco PhD student writing group, organized by Heidi Kaech, for support and accountability; Joey Bernhardt and Simon Hart for valuable discussion; and Roman Alther and Isabelle Gounand for helpful comments on manuscript drafts. This is publication ISEM-YYYY-XXX of the Institut des Sciences de l'Evolution - Montpellier. Funding is from the Swiss National Science Foundation Grants PP00P3_150698 and PP00P3_179089 and the University of Zurich Research Priority Programme *URPP Global Change and Biodiversity* (to F.A.).

Data Availability

Data will be made available on Dryad upon the manuscript's acceptance for journal publication, and until then are available on request.

References

Altermatt, F. 2013. Diversity in riverine metacommunities: a network perspective. Aquatic Ecology 47:365–377.

Altermatt, F., R. Alther, and E. Mächler. 2016. Spatial patterns of genetic diversity, community composition and occurrence of native and non-native amphipods in naturally replicated tributary streams. BMC Ecology 16:23.

Brook, B. W., and C. J. A. Bradshaw. 2006. Strength of evidence for density dependence in abundance time series of 1198 species. Ecology 87:1445–1451.

Cardinale, B. J., K. L. Matulich, D. U. Hooper, J. E. Byrnes, E. Duffy, L. Gamfeldt, P. Balvanera, et al. 2011. The functional role of producer diversity in ecosystems. American Journal of Botany 98:572–92.

Carrara, F., A. Giometto, M. Seymour, A. Rinaldo, and F. Altermatt. 2015. Experimental evidence for strong stabilizing forces at high functional diversity of aquatic microbial communities. Ecology 96:1340–1350.

Chesson, P. 2000. Mechanisms of maintenance of species diversity. Annu. Rev. Ecol. Syst 31:343–66.

———. 2012. Scale transition theory: Its aims, motivations and predictions. Ecological Complexity 10:52–68.

Dangles, O., and B. Malmqvist. 2004. Species richness-decomposition relationships depend on species dominance. Ecology Letters 7:395–402.

Denny, M., and L. Benedetti-Cecchi. 2012. Scaling Up in Ecology: Mechanistic Approaches. Annual Review of Ecology, Evolution, and Systematics 43:1–22.

Eisenhauer, N., A. D. Barnes, S. Cesarz, D. Craven, O. Ferlian, F. Gottschall, J. Hines, et al. 2016. Biodiversity–ecosystem function experiments reveal the mechanisms underlying the consequences of biodiversity change in real world ecosystems. Journal of Vegetation Science 27:1061–1070.

Gessner, M. O., C. M. Swan, C. K. Dang, B. G. McKie, R. D. Bardgett, D. H. Wall, and S. Hättenschwiler. 2010. Diversity meets decomposition. Trends in Ecology and Evolution 25:372–380.

Gounand, I., C. J. Little, E. Harvey, and F. Altermatt. 2018. Cross-ecosystem carbon flows connecting ecosystems worldwide. Nature Communications. accepted.

Grace, J. B., T. M. Anderson, E. W. Seabloom, E. T. Borer, P. B. Adler, W. S. Harpole, Y. Hautier, et al. 2016. Integrative modelling reveals mechanisms linking productivity and plant species richness. Nature 529:390–393.

Grace, J. B., T. M. Anderson, M. D. Smith, E. Seabloom, S. J. Andelman, G. Meche, E. Weiher, et al. 2007. Does species diversity limit productivity in natural grassland communities? Ecology Letters 10:680–689.

Hanski, I. 1990. Density dependence, regulation and variability in animal populations. Biological Sciences Population, Regulation, and Dynamics 330:141–150.

Harvey, L. D. D. 2000. Upscaling in global change research. Climatic change 44:225–263.

Hassell, M. P., J. H. Lawton, and R. M. May. 1976. Patterns of dynamical behavior in single species populations. Journal of Animal Ecology.

Hewitt, J. E., S. F. Thrush, P. K. Dayton, and E. Bonsdorff. 2007. The Effect of Spatial and Temporal Heterogeneity on the Design and Analysis of Empirical

Studies of Scale-Dependent Systems. The American Naturalist 169:398–408.

Hieber, M., and M. O. Gessner. 2002. Contribution of stream detrivores, fungi, and bacteria to leaf breakdown based on biomass estimates. Ecology 83:1026–1038.

Isbell, F., P. B. Reich, D. Tilman, S. E. Hobbie, S. Polasky, and S. Binder. 2013. Nutrient enrichment, biodiversity loss, and consequent declines in ecosystem productivity. Proceedings of the National Academy of Sciences 110:11911–11916.

Jonsson, M., and B. Malmqvist. 2003. Mechanisms behind positive diversity effects on ecosystem functioning: Testing the facilitation and interference hypotheses. Oecologia 134:554–559.

Kingsolver, J. G. 2009. The Well-Temperatured Biologist. The American Naturalist 174:755–768.

Klemmer, A. J., S. A. Wissinger, H. S. Greig, and M. L. Ostrofsky. 2012. Nonlinear effects of consumer density on multiple ecosystem processes. Journal of Animal Ecology 81:770–780.

Levin, S. A. 1992. The problem of pattern and scale in ecology. Ecology 73:1943–1967.

Little, C. J., and F. Altermatt. 2018*a*. Species turnover and invasion of dominant freshwater invertebrates alter biodiversity-ecosystem-function relationship. Ecological Monographs 88:461–480.

———. 2018*b*. Do priority effects outweigh environmental filtering in a guild of dominant freshwater macroinvertebrates? Proceedings of the Royal Society B: Biological Sciences 285.

MacNeil, C., P. Boets, and D. Platvoet. 2012. “Killer shrimps”, dangerous experiments and misguided introductions: how freshwater shrimp (Crustacea:

Amphipoda) invasions threaten biological water quality monitoring in the British Isles. Freshwater Reviews 5:21–35.

McPeek, M. A. 2012. Intraspecific density dependence and a guild of consumers coexisting on one resource. Ecology 93:2728–2735.

Melbourne, B. A., and P. Chesson. 2005. Scaling up population dynamics: Integrating theory and data. Oecologia 145:179–187.

Patrick, C. J. 2013. The effect of shredder community composition on the production and quality of fine particulate organic matter. Freshwater Science 32:1026–1035.

Pebesma, E. J. 2004. Multivariable geostatistics in S: the gstat package. Computers and Geosciences 30:683–691.

Pinheiro, J., D. Bates, S. DebRoy, D. Sarkar, and R Core Development Team. 2013. nlme: Linear and nonlinear mixed effects models.

Piscart, C., F. Mermillod-Blondin, C. Maazouzi, S. Merigoux, and P. Marmonier. 2011. Potential impact of invasive amphipods on leaf litter recycling in aquatic ecosystems. Biological Invasions 13:2861–2868.

Ruel, J. J., and M. P. Ayres. 1999. Jensen's inequality predicts effects of environmental variation. Trends in Ecology and Evolution 5347:361–366.

Schoener, T. W. 1983. Field experiments on interspecific competition. American Naturalist 122:240–285.

Snelgrove, P. V. R., S. F. Thrush, D. H. Wall, and A. Norkko. 2014. Real world biodiversity-ecosystem functioning: A seafloor perspective. Trends in Ecology and Evolution 29:398–405.

Swisstopo. 2007. Vector 25 Gewässernetz. 5704 000 000, reproduced by permission of swisstopo / JA100119, Bundesamt für Landestopographie (Art.30 Geo IV).

———. 2010. Vector 25. 5704 000 000, reproduced by permission of swisstopo / JA100119, Bundesamt für Landestopographie (Art.30 Geo IV).

———. 2014. swissTLM3D. 5704 000 000, reproduced by permission of swisstopo / JA100119, Bundesamt für Landestopographie (Art.30 Geo IV).

Tilman, D., F. Isbell, and J. M. Cowles. 2014. Biodiversity and ecosystem functioning. Annual Review of Ecology, Evolution, and Systematics 45:471–493.

Van den Brink, F. W. B., G. Van der Velde, and A. Bij de Vaate. 1991. Amphipod invasion on the Rhine. Nature 352:576.

Wardle, D. A. 2016. Do experiments exploring plant diversity-ecosystem functioning relationships inform how biodiversity loss impacts natural ecosystems? Journal of Vegetation Science 27:646–653.

Weis, J. J., B. J. Cardinale, K. J. Forshay, and A. R. Ives. 2007. Effects of Species Diversity on Community Biomass Production Change Over the Course of Succession. Ecology 88:929–939.

Welton, J. S. 1979. Life-history and production of the amphipod *Gammarus pulex* in a Dorset chalk stream. Freshwater Biology 9:263–275.

Tables

Table 1. Total amphipod abundance estimated using inverse distance weighted interpolation based on field sampling (*n* = number of sampling points in catchment, *l* = total stream length in the catchment), and two different upscaled estimates to whole-catchment leaf litter processing rates (grams/day). Briefly, Scenario 1 assumes density-independent per-capita processing; Scenario 2 assumes spatially-varying abundances and density-dependent leaf consumption calculated for each stream reach based on its particular abundance. Estimates are means of 1000 simulations, with 95% confidence intervals shown in parentheses.

Stream name	Total Abundance	Scenario 1 Processing	Scenario 2 Processing
Chesselbach *n = 13, l = 4.5 km*	720,719 *(± 1,035)*	8,194.7 *(± 122.1)*	315.4 (± 0.5)
Dorfbach *n = 15, l = 4.3 km*	808 *(± 6)*	9.2 *(± 0.3)*	9.8 (± 0.1)
Eschlibach *n = 12, l = 4.1 km*	1,135,006 *(±1,249)*	12,905.2 *(± 145.9)*	312.6 (± 0.49)
Hepbach *n = 13, l = 3.8 km*	231,020 *(±622)*	2,626.7 *(± 67.6)*	178.3 (± 0.7)
Imbersbach *n = 11, l = 3.3 km*	139,222 *(±613)*	1,583.0 *(± 45.1)*	119.0 (± 1.2)
Mannenbach *n = 15, l = 4.8 km*	1,464,130 *(±1,408)*	16,647.4 *(± 178.1)*	378.0 (± 0.6)
Seebach *n = 11, l = 3.2 km*	1,370,115 *(±1,250)*	15,578.4 *(± 139.1)*	260.4 (± 0.3)
Tobelmühlibach *n = 12, l = 3.7 km*	696,563 *(±1,081)*	7,920.0 *(± 107.8)*	239.9 (± 0.5)
Unnamed Stream 1 *n = 9, l = 2.8 km*	518,543 *(±849)*	5,895.9 *(± 120.8)*	172.1 (± 0.6)
Unnamed Stream 2 *n = 10, l = 3.6 km*	317,053 *(±672)*	3,604.9 *(± 64.2)*	234.3 (± 0.4)

Figures

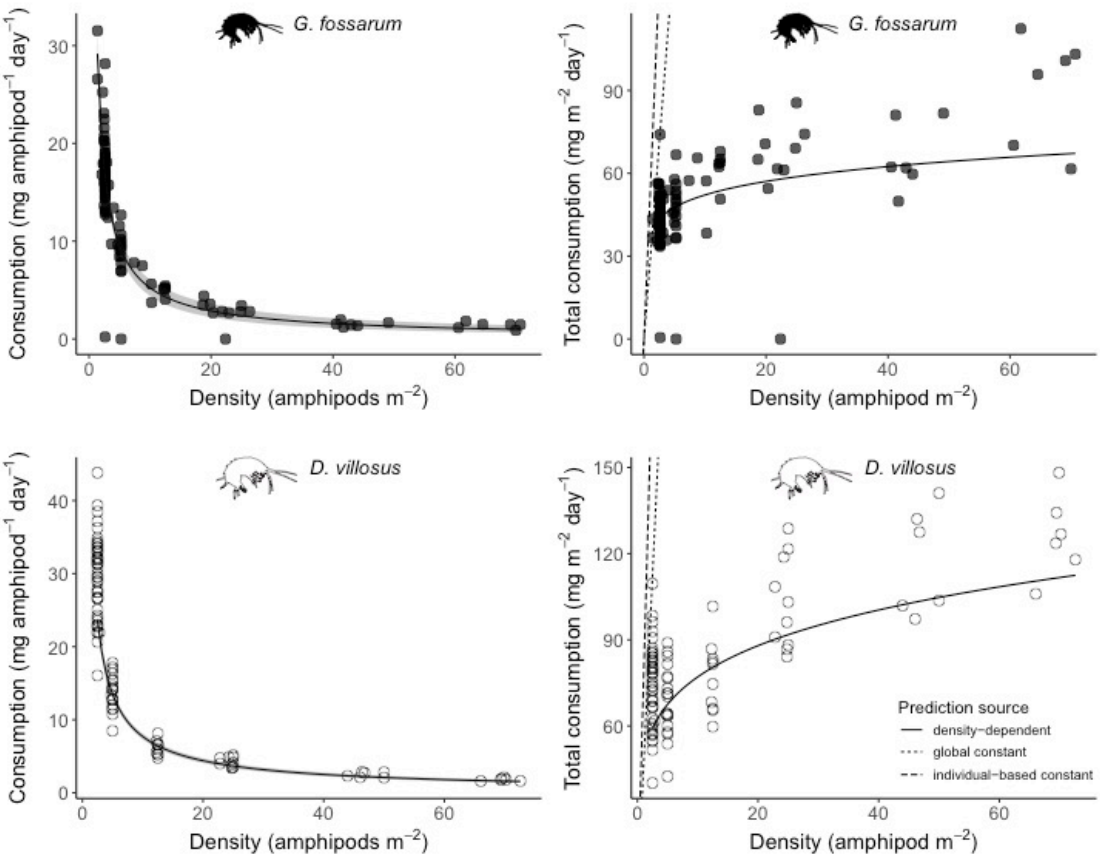

Figure 1. Negative exponential relationships (left panels) between density and per-capita consumption rates for *G. fossarum* (consumption = 38.6*density$^{-0.87}$) and *D. villosus* (consumption = 49.7*density$^{-0.81}$) in mesocosm experiments. Gray shading shows the 95% confidence interval of the model fit. Right panels show the total daily leaf litter consumption per mesocosm, overlaid by expected values from the negative exponential functions derived at left (solid lines), constant per-capita consumption rates calculated by averaging all mesocosms (dotted line), and constant per-capita consumption rates calculated only from mesocosms with one individual amphipod each (dashed line). Note the different x- and y-axis ranges for the two species.

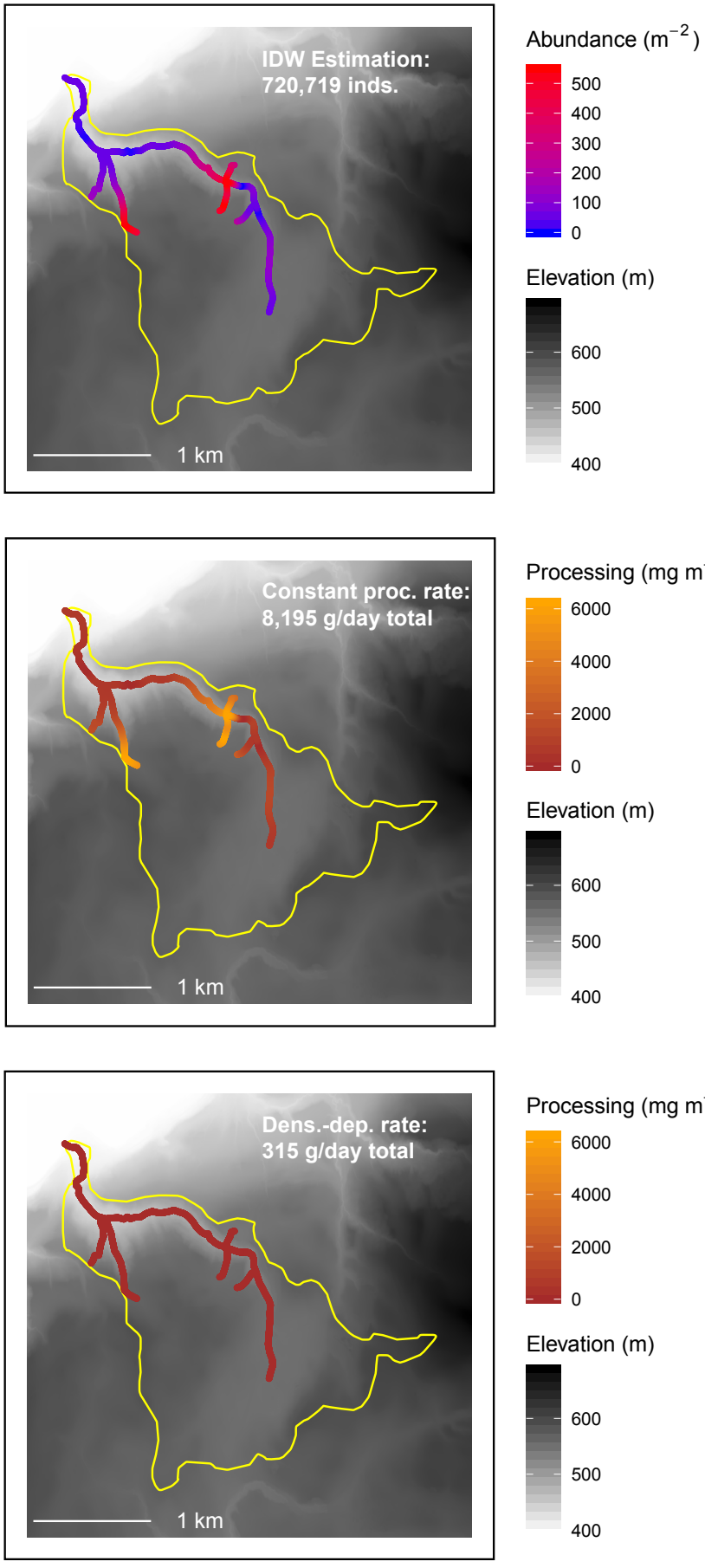

Figure 2. Hotspots of abundance (top panel) and leaf litter processing (bottom panels) in the Chesselbach stream catchment (outlined in yellow), based on upscaling abundance data from 13 sampling points up to longitudinal abundance distributions using inverse distance weighted interpolation. Daily processing rates were calculated by multiplying the interpolated abundance in a 1 m section of stream length by either the average per capita consumption rate of *G. fossarum* (middle panel) or the experimentally-derived negative power function relating *G. fossarum* density to per-capita leaf litter consumption (bottom panel). This figure shows the mean of 1000 simulations of the interpolation process. Because stream reaches with higher densities of individuals have the lowest per-capita processing rates, the spatial distribution of leaf litter processing under this scenario is very different than the spatial distribution of amphipod abundance, with the effect of homogenizing ecosystem function in space despite having heterogeneous biomass. Data sources: swisstopo (2010, 2014), Vector25 and TLM3D, DV 5704 000 000, reproduced by permission of swisstopo/JA100119.

Supplementary Material

Methods

Experimental details

The experiments were first performed on *Gammarus fossarum* in November 2016. We collected *G. fossarum* by kicknet from Sagentobelbach in Dübendorf, Switzerland (47.39° N, 8.59° W). Only adults were brought to the laboratory, where they were placed in large holding containers of ~500 individuals, gradually brought up to 18 °C, and acclimated for two and a half days with ad libitum alder (*Alnus glutinosa* (Gaertner)) leaves conditioned for six days in stream water to establish natural microbial and fungal communities. In January 2017, we repeated the experiment with *D. villosus* individuals collected by kicknet from Lake Constance at Kesswil, Switzerland (47.60° N, 9.32° W).

For both focal species, we distributed individuals into experimental units so that medium and large individuals were equally represented in all replicates. With respect to sex, unless one divides individuals into males and females by separating precopulatory pairs, a microscope is necessary to identify sex. This is impractical in the field, and handling can injure the individuals. We instead assumed that subsequent allocation of individuals to treatments was random across the experiment.

Data exploration and analysis

Because the measures of density had long right tails, we explored density-consumption relationships which log-transformed this variable. We first used linear models to create (1) simple linear models, (2) linear models with log-transformed density data, and (3) linear models with log-transformed density and log-transformed consumption data. For this analysis, any zero values of consumption were replaced

with 0.01 to enable log-transformation; fitting of nonlinear models (see below) used original data with zeros. To determine which type of model best fit the data, we examined diagnostic plots and tested each model's residuals for normality using a Shapiro-Wilkes test. Non-normal residuals taken to indicate poor model fit, and we planned to use this initial comparison to determine which of three strategies to use for fitting the data: (1) if simple linear models had residuals that met assumptions of normality and homoscedasticity, we would use these models; (2) if the models with log-transformed density fit best we would re-fit the data using generalized linear models (GLM) with a log link function, and (3) if the third models fit best we would re-fit the data using non-linear least square models (NLS). However, we used normality of residuals in combination with other diagnostics to determine the best model for the data. Data were linear in log-log space for both species (Figure S1).

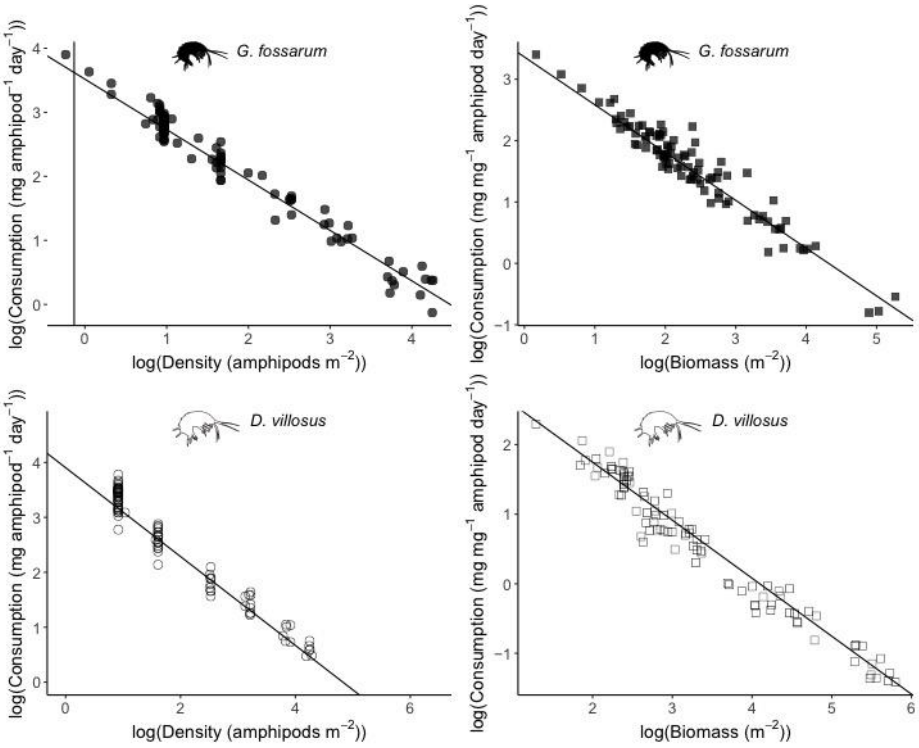

Figure S1. The association between density and per-capita consumption rate is linear in log-log space, for both *G. fossarum* and *D. villosus*, and both when measuring density as individual abundance or as biomass.

For *G. fossarum,* the simple linear model (scenario 1 above) was the only model with normal residuals (Table S1). However, diagnostics indicated that this model did not fit the data well (Figure S2).

Table S1. In order to determine the shape of the density-consumption relationship, residuals of different models (linear-linear, linear-log, and log-log) were tested for normality using a Shapiro-Wilkes test, where the null hypothesis is normality of the distribution. The *G. fossarum* dataset comprised 97 observations, and the *D. villosus* dataset 96 observations.

Model specification	**Shapiro W statistic**	**Shapiro p-value**	**Model Adjusted R^2**
G. fossarum, individual density			
consumption ~ density	0.98	0.09	0.45
consumption ~ log(density)	0.92	< 0.001	0.73
log(consumption) ~ log(density)	0.31	< 0.001	0.45
G. fossarum, biomass density			
consumption ~ density	0.59	< 0.001	0.13
consumption ~ log(density)	0.63	< 0.001	0.52
log(consumption) ~ log(density)	0.37	< 0.001	0.44
D. villosus, individual density			
consumption ~ density	0.94	< 0.001	0.46
consumption ~ log(density)	0.97	0.04	0.77
log(consumption) ~ log(density)	0.98	0.30	0.96
D. villosus, biomass density			
consumption ~ density	0.90	< 0.001	0.37
consumption ~ log(density)	0.94	< 0.001	0.73
log(consumption) ~ log(density)	0.98	0.21	0.96

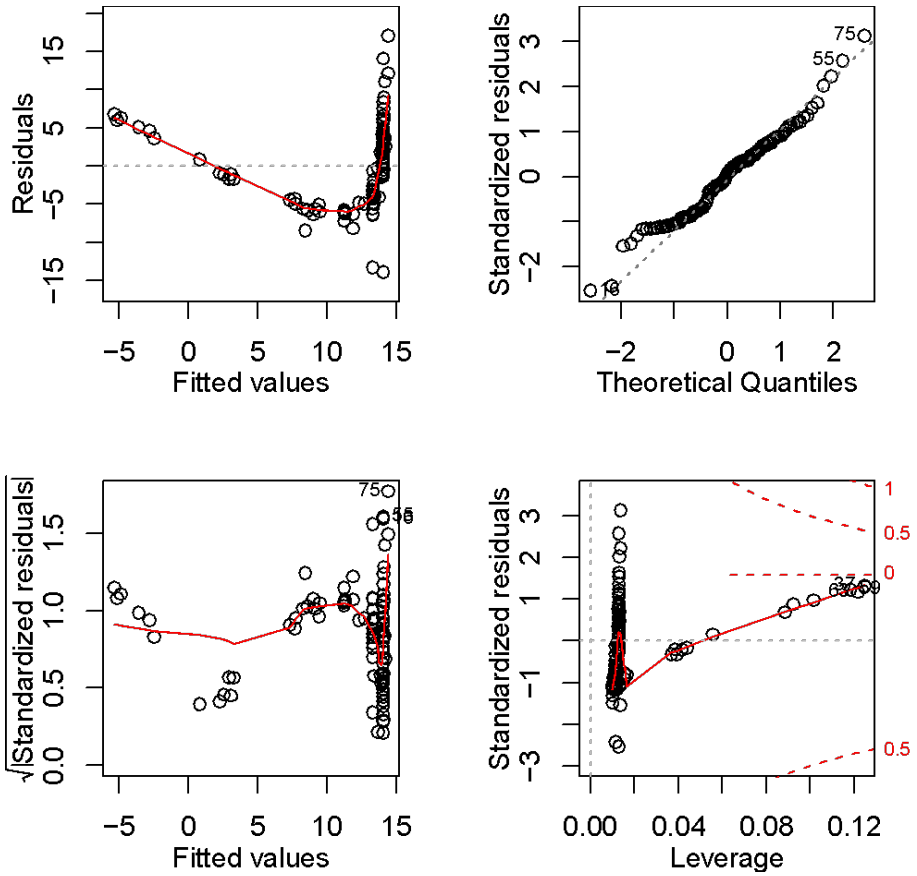

Figure S2. Diagnostic plots for the simple linear model of per-amphipod consumption rates as a function of density.

While the residuals of the third model (on log-transformed density and consumption data) did not meet the assumption of normality according to the Shapiro-Wilkes test (Table S1), the other diagnostics indicate that the log-log model fit the data best other than three outliers where no leaf litter had been consumed (Figure S3).

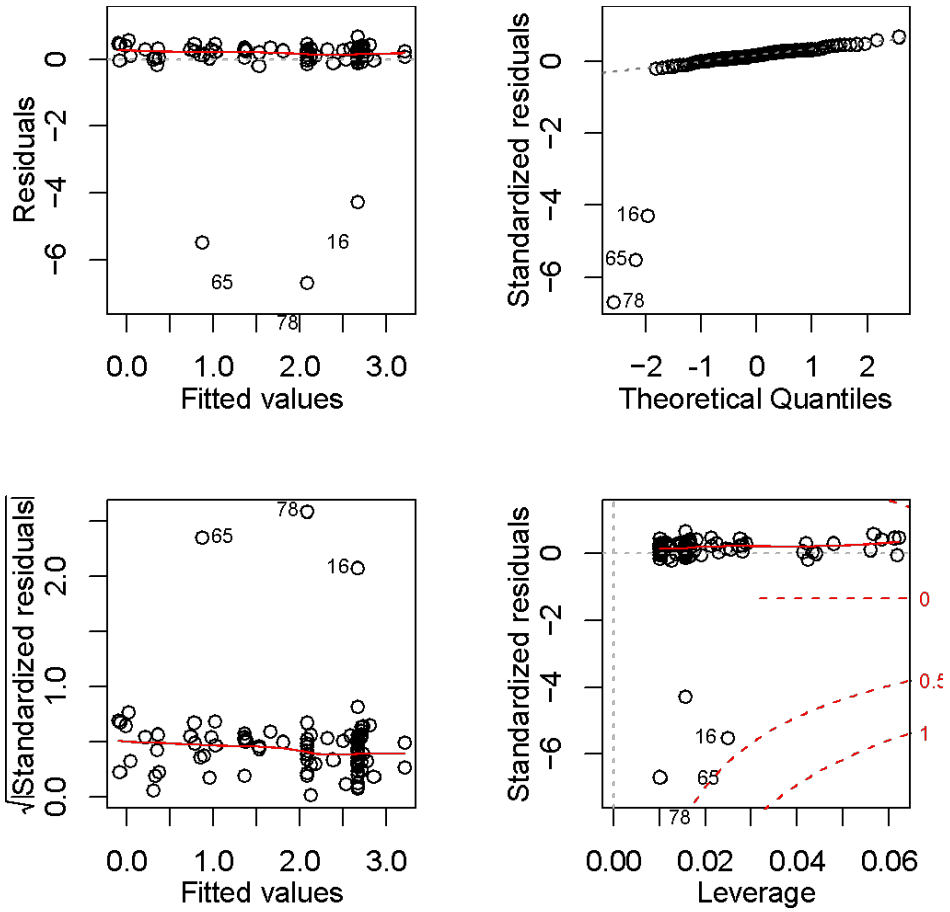

Figure S3. Diagnostic plots for the linear model of log-transformed per-amphipod consumption rates as a function of log-transformed density.

While deviating from normality, these observations did not have such high leverage (Cook's distance, red lines in Figure S3) to exclude them, and would only make the nonlinear fit estimates more conservative by pulling down estimated consumption rates at low densities (Figure 1). Thus, we chose nonlinear model fits for both species.

For the *D. villosus*, only the third linear model scenario (with log transformed density and consumption data) had normal residuals (see Table S1 above).

Therefore, we developed NLS models for both species. Parameter estimates from the linear models of transformed data were used as starting values for the NLS models. 95% confidence intervals for the model fits were generated by making 100,000 samples of coefficient estimates based on the approximate variance-covariance matrix extracted from the gNLS.

Results

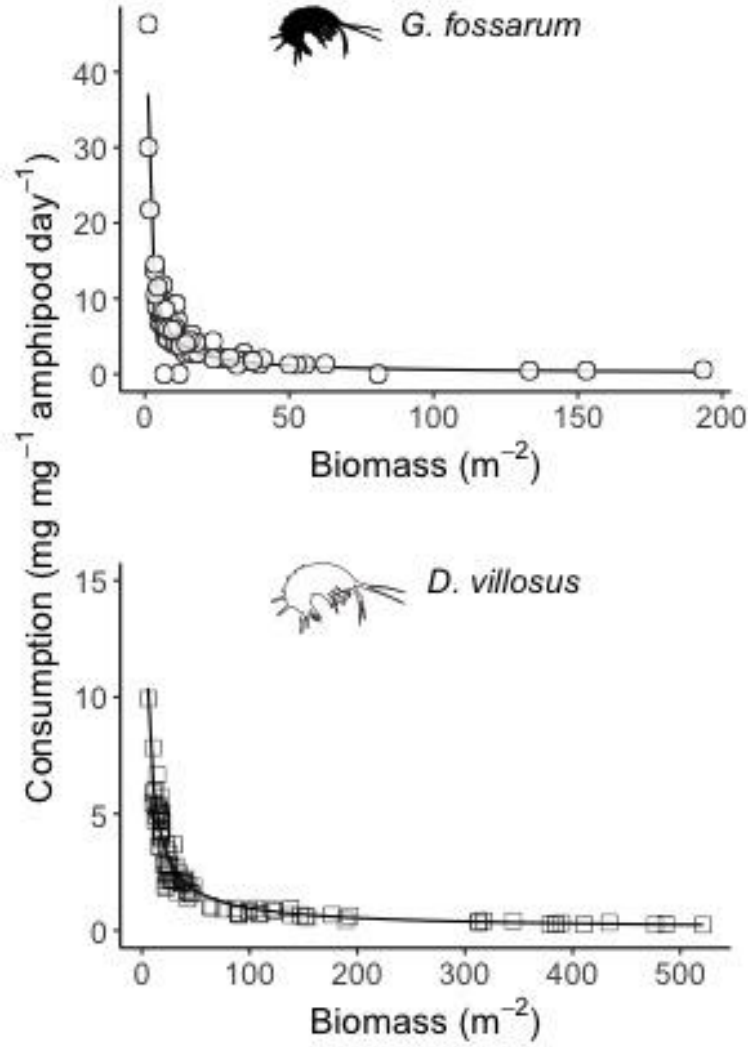

Figure S4. Negative exponential relationships between biomass and leaf litter consumption rates in experimental mesocosms for *G. fossarum* (consumption = 40.3*biomass$^{-0.92}$) and *D. villosus* (consumption=44.7*biomass$^{-0.83}$).

Table S2. Total amphipod abundance estimated using proportional estimation based on field sampling (n = number of sampling points in catchment, l = total stream length in the catchment), and three different upscaled estimates to whole-catchment leaf litter processing rates (grams/day). Briefly, Scenario 1 assumes density-independent per-capita processing; Scenario 2 assumes spatially-varying abundances in a catchment with leaf consumption calculated for each stream reach based on its particular abundance. Estimates are means of 1000 simulations, with 95% confidence intervals shown in parentheses.

Stream name	Total Abundance	Scenario 1 Processing	Scenario 2 Processing
Chesselbach *n = 13, l = 4.5 km*	*692,825* *(± 1,035)*	*7,877.5* *(± 11.8)*	272.2 *(± 0.1)*
Dorfbach *n = 15, l = 4.3 km*	*1,587* *(± 6)*	*18.0* *(± 0.1)*	*13.6* *(± 0.0)*
Eschlibach *n = 12, l = 4.1 km*	*1,179,563* *(± 1,249)*	*13,411.8* *(± 14.2)*	*272.6* *(± 0.1)*
Hepbach *n = 13, l = 3.8 km*	*186,550* *(± 622)*	*2,121.1* *(± 7.1)*	*139.3* *(± 0.1)*
Imbersbach *n = 11, l = 3.3 km*	*166,930* *(± 613)*	*1,898.0* *(± 7.0)*	*53.7* *(± 0.1)*
Mannenbach *n = 15, l = 4.8 km*	*1,351,796* *(± 1,408)*	*15,370.1* *(± 16.0)*	*334.3* *(± 0.1)*
Seebach *n = 11, l = 3.2 km*	*1,434,449* *(± 1,250)*	*16,309.9* *(± 14.2)*	*250.1* *(± 0.1)*
Tobelmühlibach *n = 12, l = 3.7 km*	*738,789* *(± 1,081)*	*8,400* *(± 12.3)*	*183.4* *(± 0.1)*
Unnamed Stream 1 *n = 9, l = 2.8 km*	*361,717* *(± 849)*	*4,112.8* *(± 9.6)*	*74.0* *(± 0.1)*
Unnamed Stream 2 *n = 10, l = 3.6 km*	*322,401* *(± 672)*	*3,665.7* *(± 7.6)*	*220.1* *(± 0.0)*

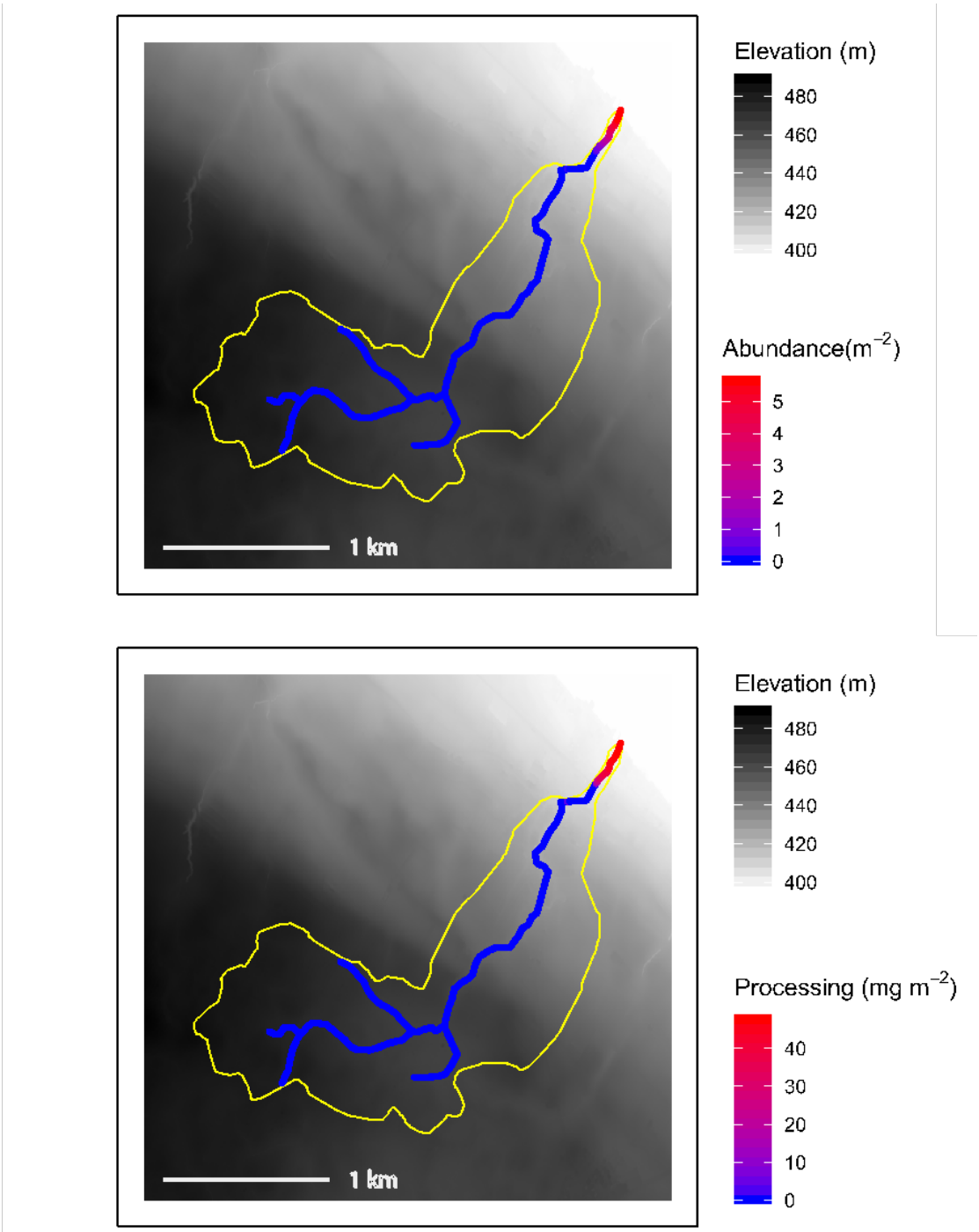

Figure S5. Hotspots of abundance (top panel) and leaf litter processing (bottom panel) in the Dorfbach stream catchment (outlines in yellow), based on upscaling abundance data from 15 sampling points up to longitudinal abundance distributions using inverse distance weighted interpolation. Processing rates (per day) were calculated by multiplying the interpolated abundance in a 1 m section of stream length by the experimentally-derived negative power relating *G. fossarum* density to per-capita leaf litter consumption. This figure shows the mean of 1000 simulations of the interpolation process. Data sources: swisstopo (2010, 2014), Vector25 and TLM3D, DV 5704 000 000, reproduced by permission of swisstopo/JA100119.

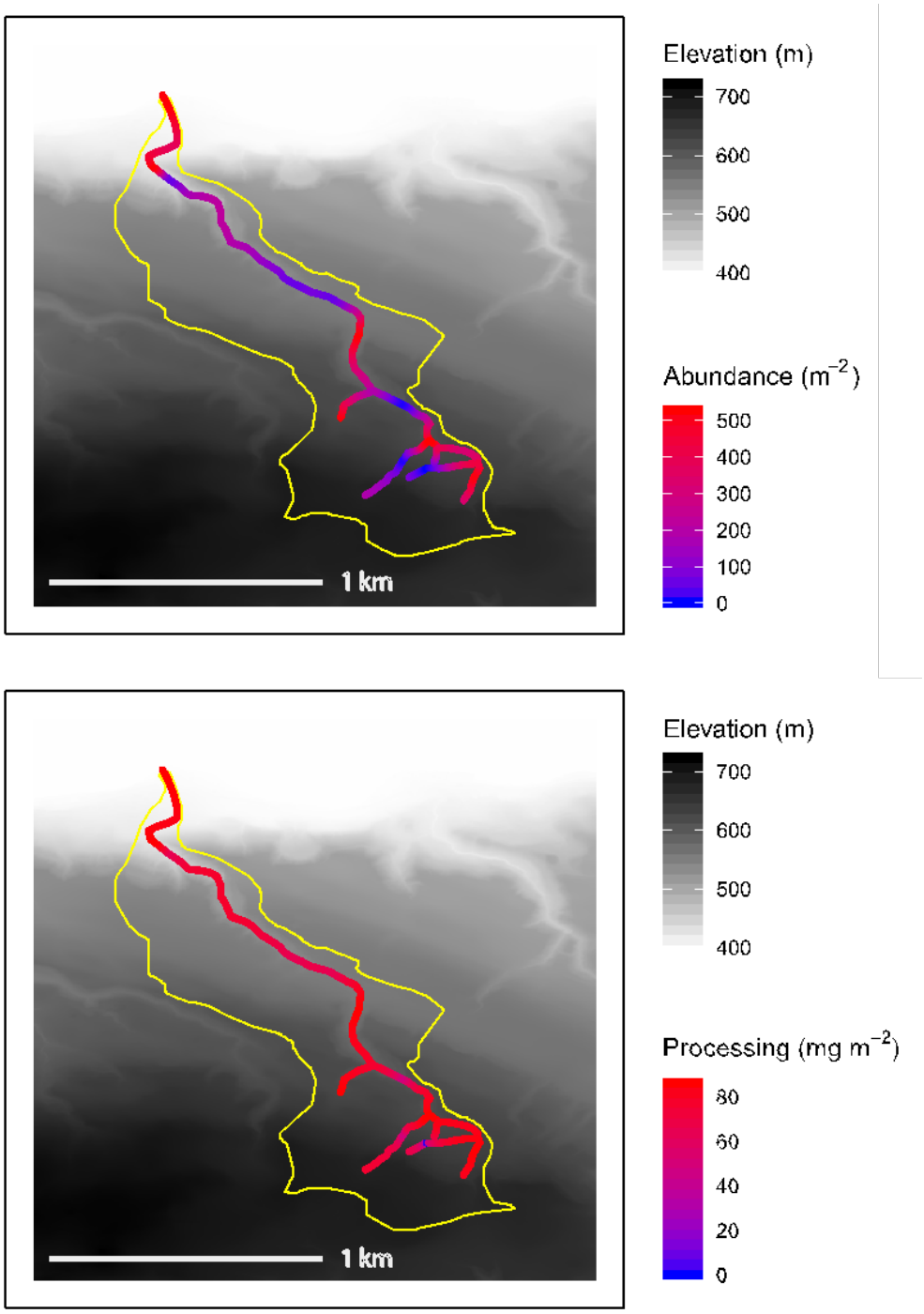

Figure S6. Hotspots of abundance (top panel) and leaf litter processing (bottom panel) in the Eschlibach stream catchment (outlines in yellow), based on upscaling abundance data from 12 sampling points up to longitudinal abundance distributions using inverse distance weighted interpolation. Processing rates (per day) were calculated by multiplying the interpolated abundance in a 1 m section of stream length by the experimentally-derived negative power relating *G. fossarum* density to per-capita leaf litter consumption. This figure shows the mean of 1000 simulations of the interpolation process. Data sources: swisstopo (2010, 2014), Vector25 and TLM3D, DV 5704 000 000, reproduced by permission of swisstopo/JA100119.

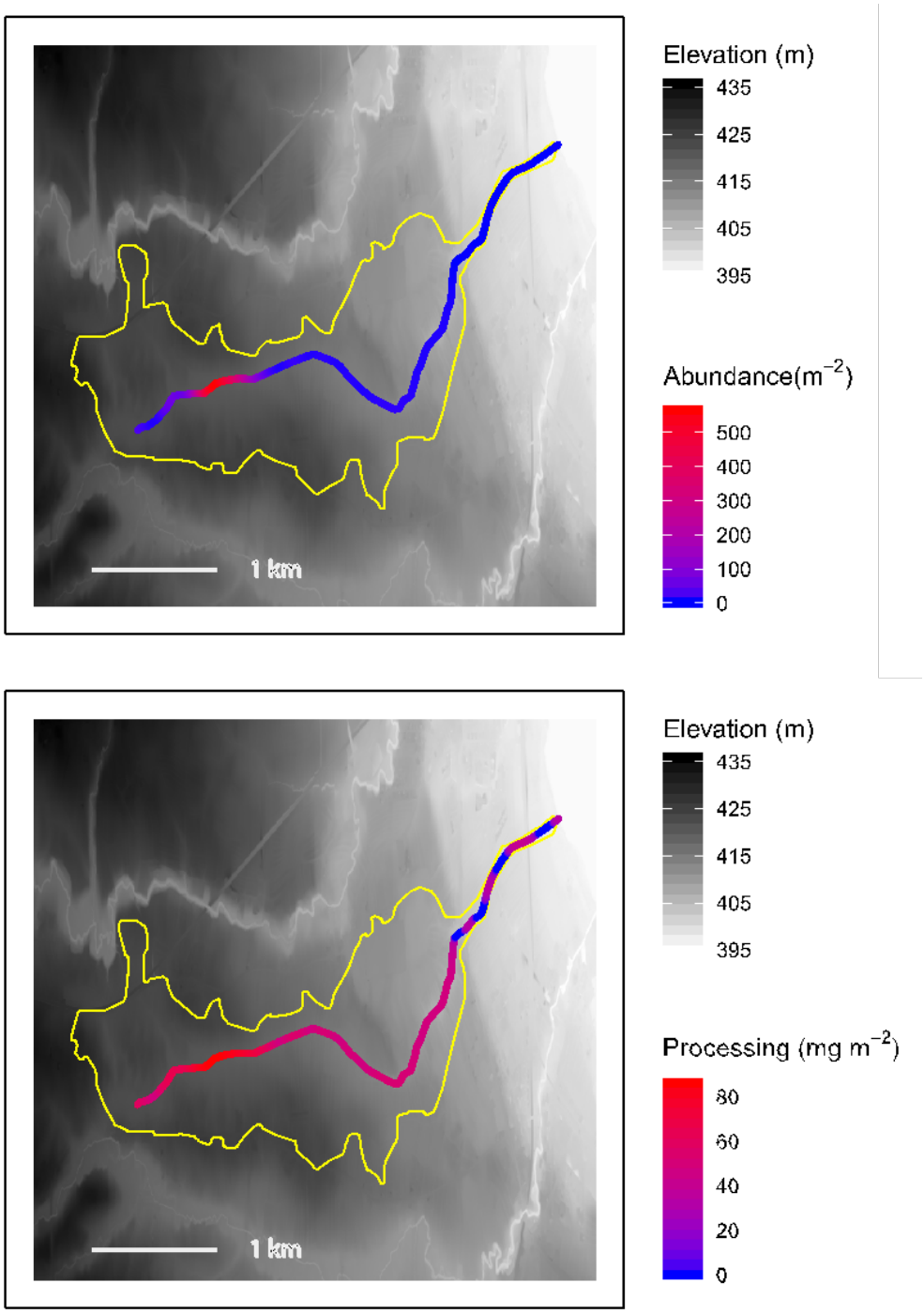

Figure S7. Hotspots of abundance (top panel) and leaf litter processing (bottom panel) in the Hepbach stream catchment (outlines in yellow), based on upscaling abundance data from 13 sampling points up to longitudinal abundance distributions using inverse distance weighted interpolation. Processing rates (per day) were calculated by multiplying the interpolated abundance in a 1 m section of stream length by the experimentally-derived negative power relating *G. fossarum* density to per-capita leaf litter consumption. This figure shows the mean of 1000 simulations of the interpolation process. Data sources: swisstopo (2010, 2014), Vector25 and TLM3D, DV 5704 000 000, reproduced by permission of swisstopo/JA100119.

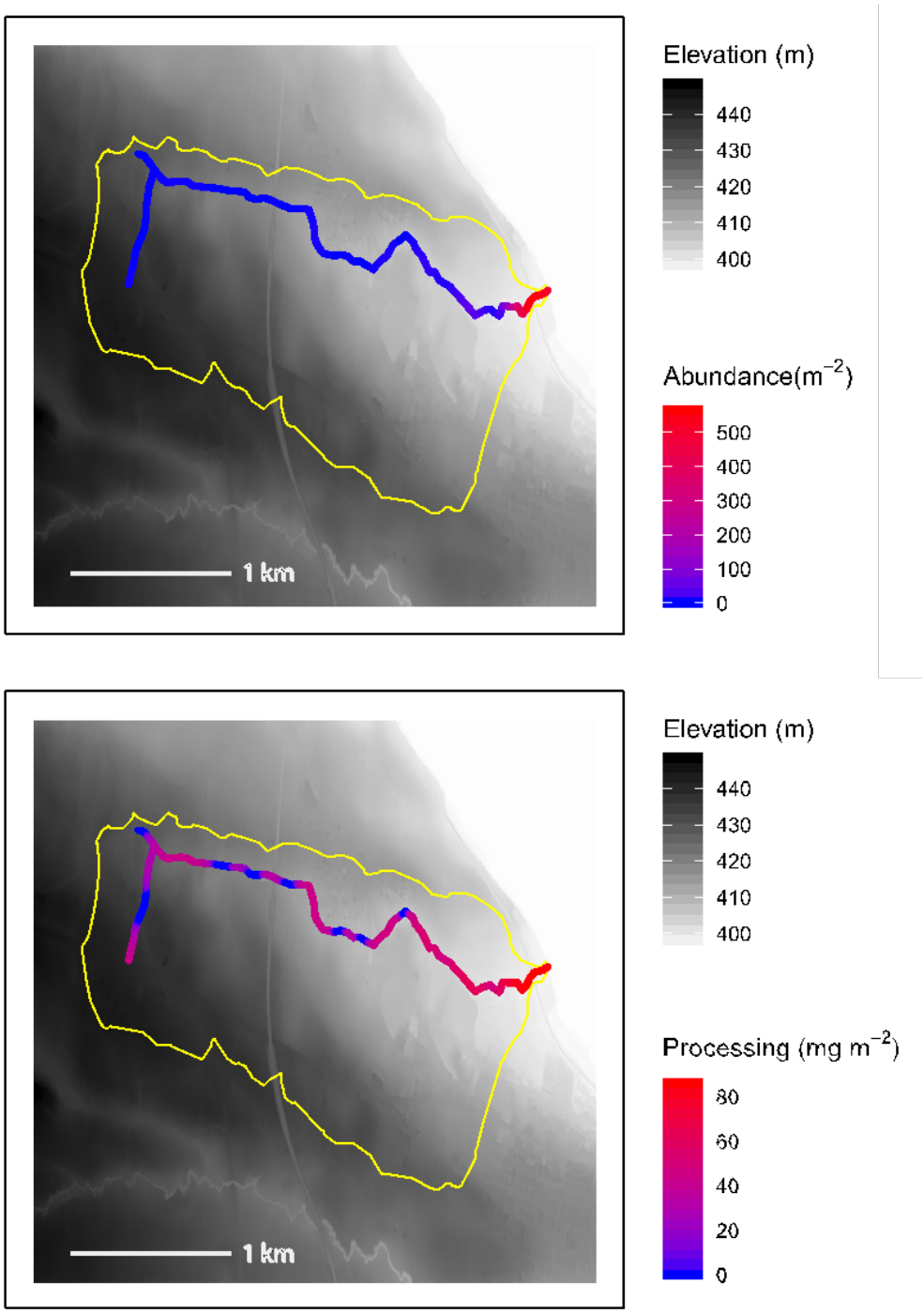

Figure S8. Hotspots of abundance (top panel) and leaf litter processing (bottom panel) in the Imbersbach stream catchment (outlines in yellow), based on upscaling abundance data from 11 sampling points up to longitudinal abundance distributions using inverse distance weighted interpolation. Processing rates (per day) were calculated by multiplying the interpolated abundance in a 1 m section of stream length by the experimentally-derived negative power relating *G. fossarum* density to per-capita leaf litter consumption. This figure shows the mean of 1000 simulations of the interpolation process. Data sources: swisstopo (2010, 2014), Vector25 and TLM3D, DV 5704 000 000, reproduced by permission of swisstopo/JA100119.

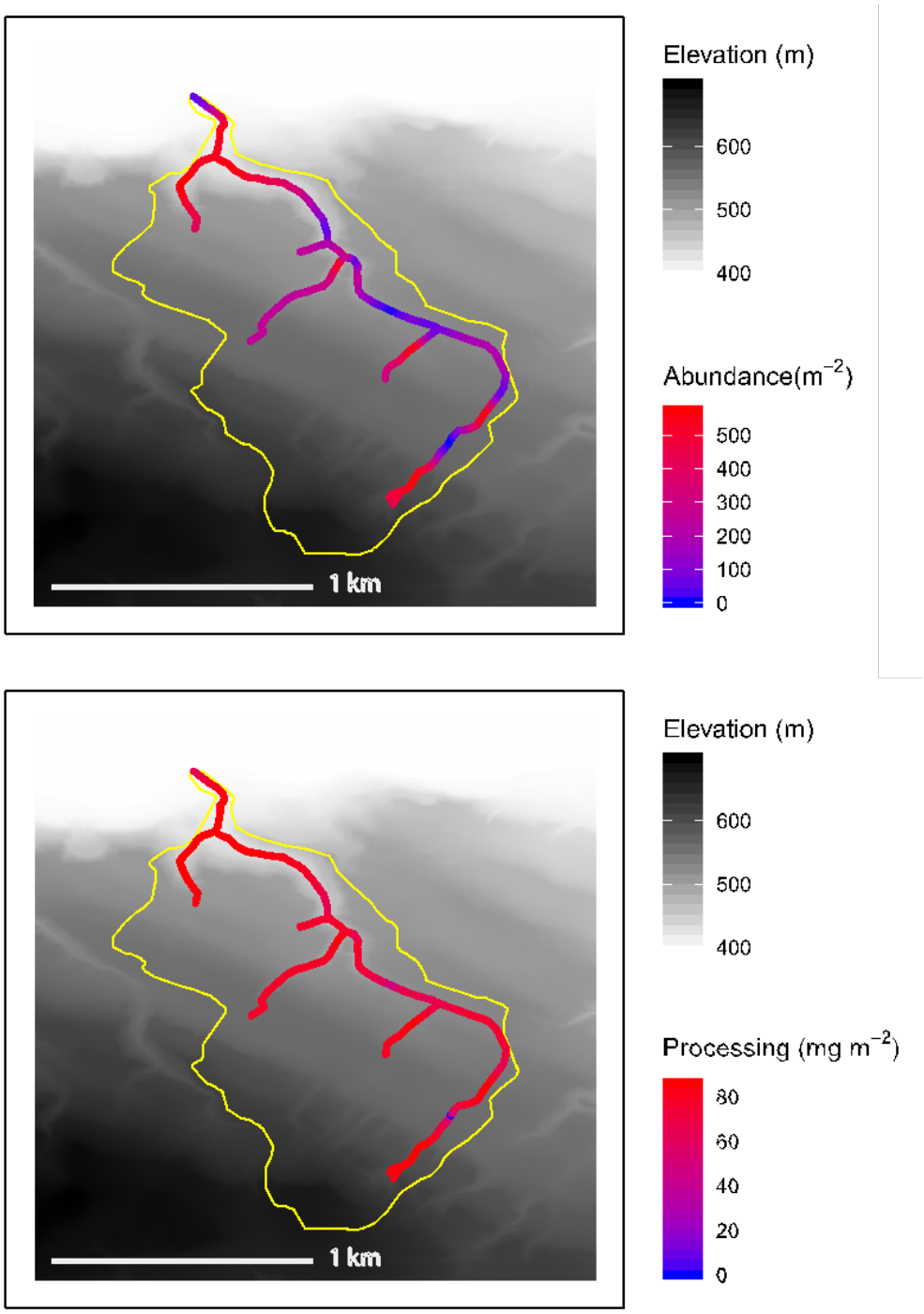

Figure S9. Hotspots of abundance (top panel) and leaf litter processing (bottom panel) in the Mannenbach stream catchment (outlines in yellow), based on upscaling abundance data from 15 sampling points up to longitudinal abundance distributions using inverse distance weighted interpolation. Processing rates (per day) were calculated by multiplying the interpolated abundance in a 1 m section of stream length by the experimentally-derived negative power relating *G. fossarum* density to per-capita leaf litter consumption. This figure shows the mean of 1000 simulations of the interpolation process. Data sources: swisstopo (2010, 2014), Vector25 and TLM3D, DV 5704 000 000, reproduced by permission of swisstopo/JA100119.

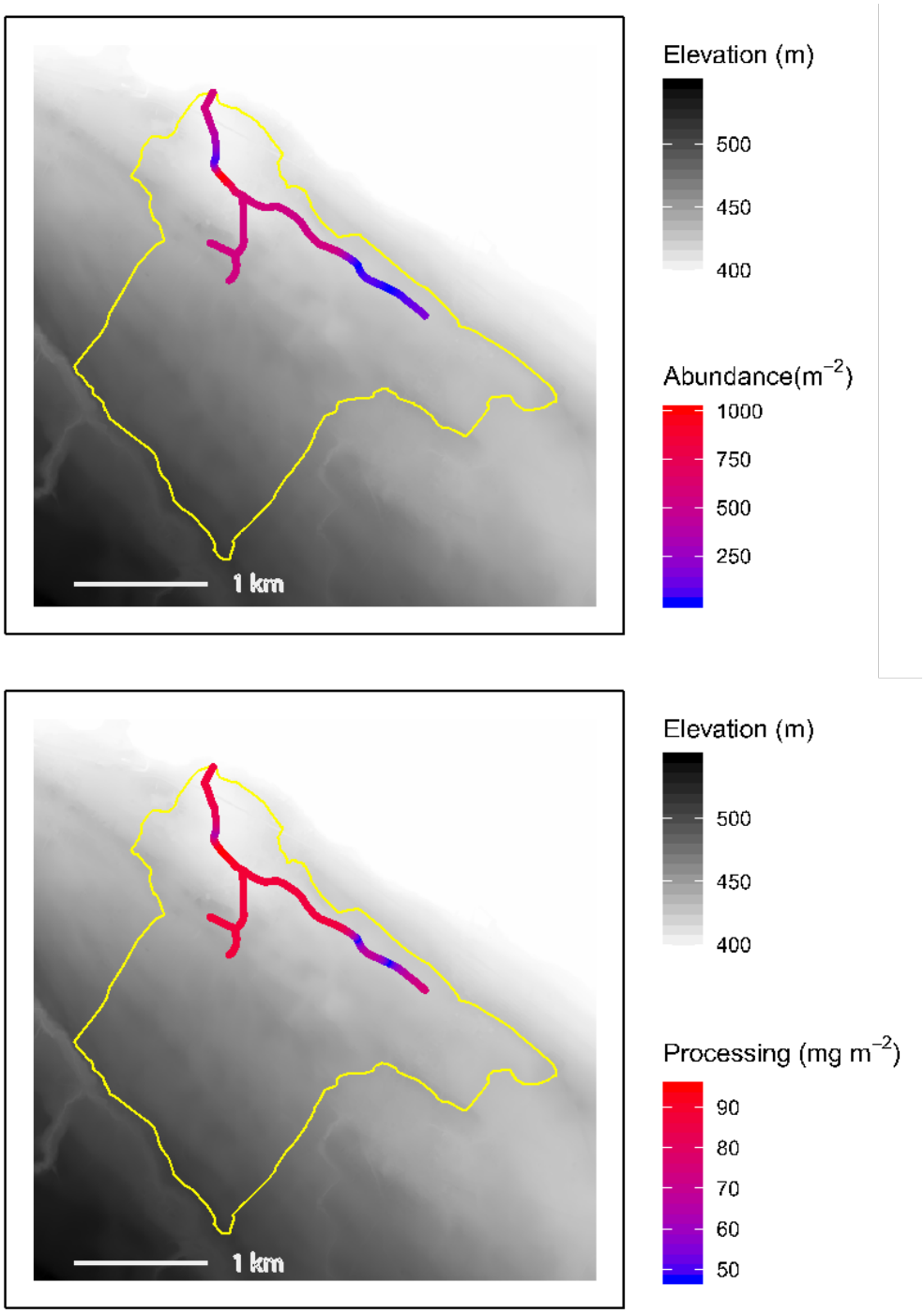

Figure S10. Hotspots of abundance (top panel) and leaf litter processing (bottom panel) in the Seebach stream catchment (outlines in yellow), based on upscaling abundance data from 11 sampling points up to longitudinal abundance distributions using inverse distance weighted interpolation. Processing rates (per day) were calculated by multiplying the interpolated abundance in a 1 m section of stream length by the experimentally-derived negative power relating *G. fossarum* density to per-capita leaf litter consumption. This figure shows the mean of 1000 simulations of the interpolation process. Data sources: swisstopo (2010, 2014), Vector25 and TLM3D, DV 5704 000 000, reproduced by permission of swisstopo/JA100119.

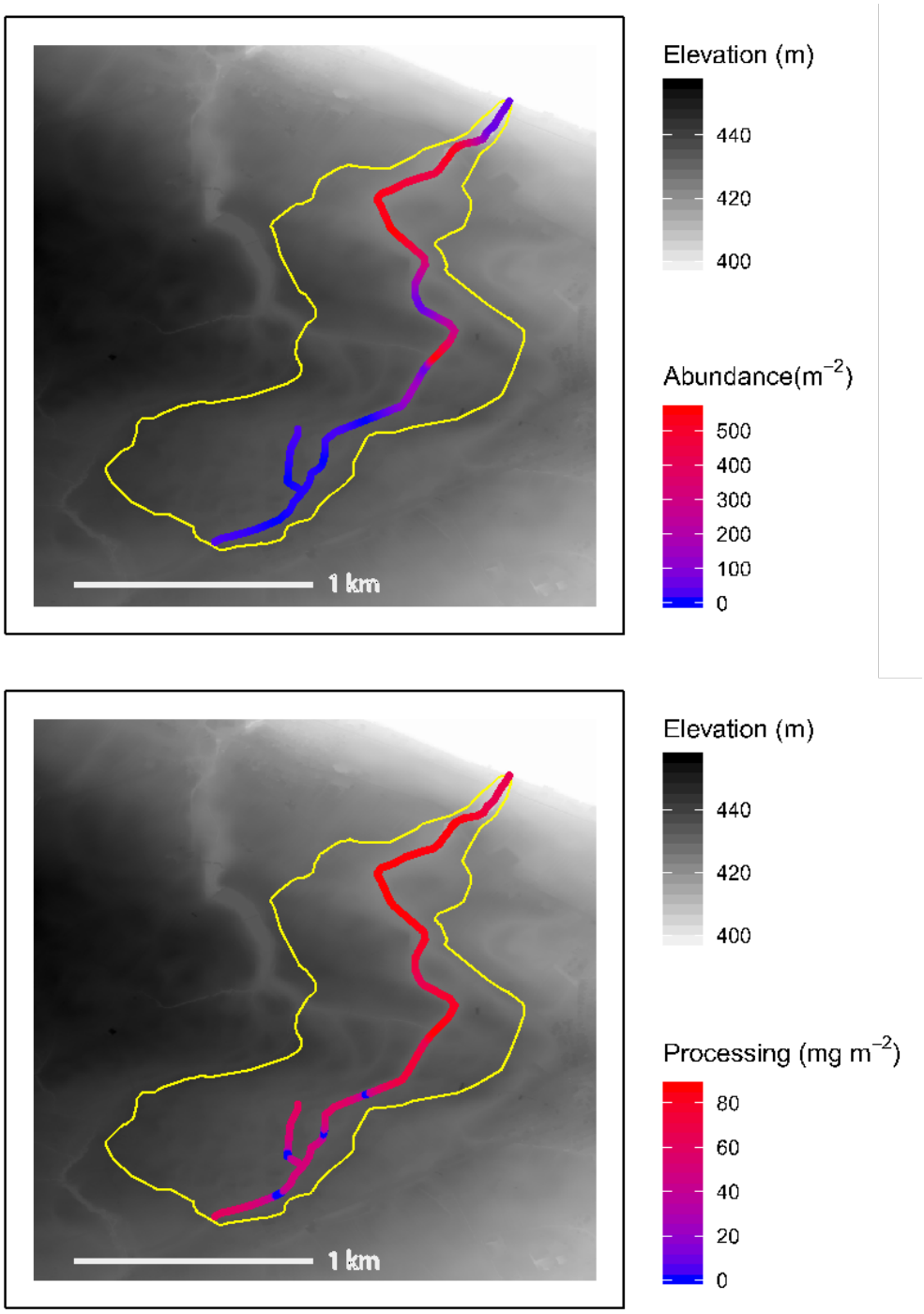

Figure S11. Hotspots of abundance (top panel) and leaf litter processing (bottom panel) in the Tobelmühlibach stream catchment (outlines in yellow), based on upscaling abundance data from 12 sampling points up to longitudinal abundance distributions using inverse distance weighted interpolation. Processing rates (per day) were calculated by multiplying the interpolated abundance in a 1 m section of stream length by the experimentally-derived negative power relating *G. fossarum* density to per-capita leaf litter consumption. This figure shows the mean of 1000 simulations of the interpolation process. Data sources: swisstopo (2010, 2014), Vector25 and TLM3D, DV 5704 000 000, reproduced by permission of swisstopo/JA100119.

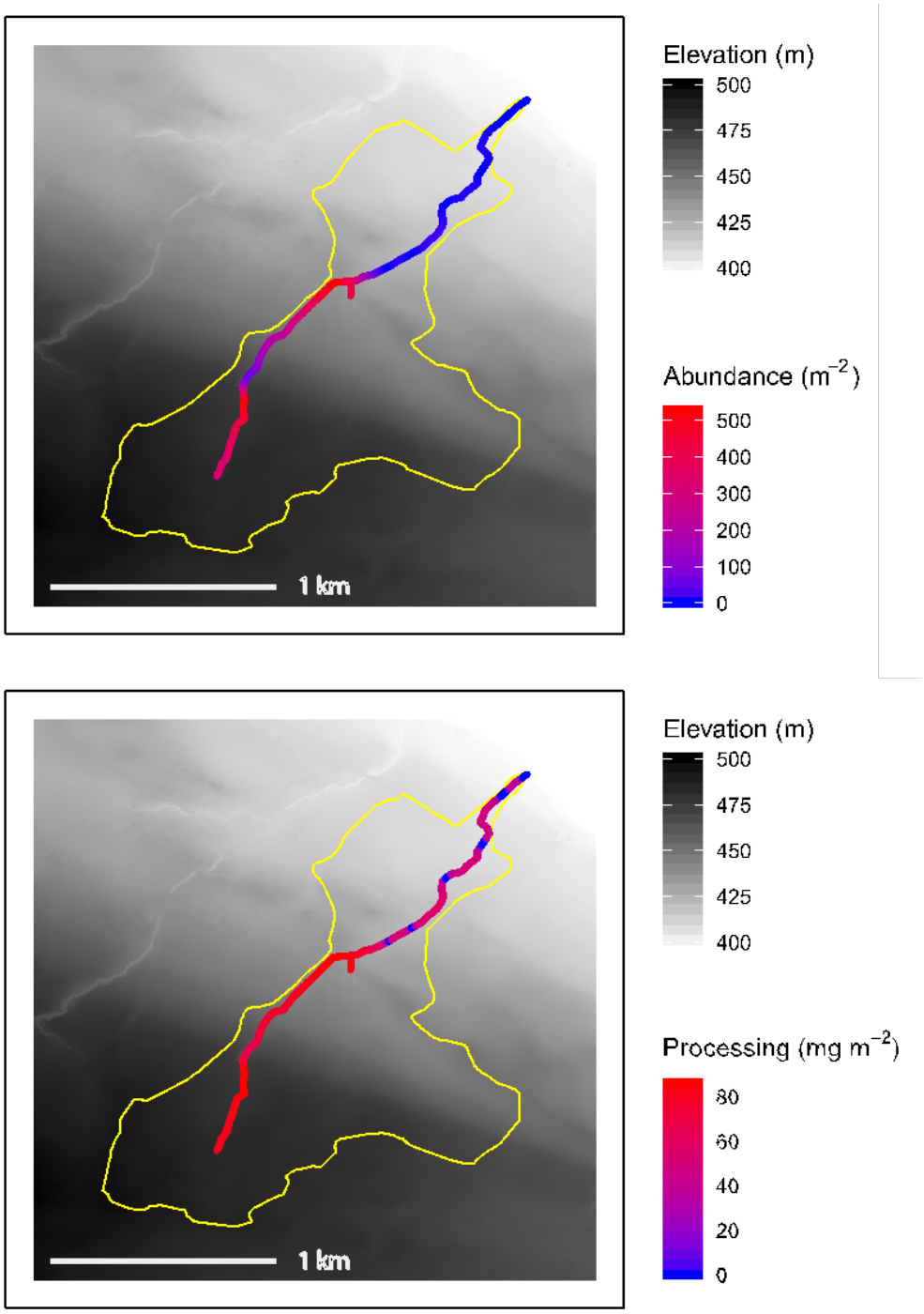

Figure S12. Hotspots of abundance (top panel) and leaf litter processing (bottom panel) in the Unnamed Stream #1 catchment (outlines in yellow), based on upscaling abundance data from 9 sampling points up to longitudinal abundance distributions using inverse distance weighted interpolation. Processing rates (per day) were calculated by multiplying the interpolated abundance in a 1 m section of stream length by the experimentally-derived negative power relating *G. fossarum* density to per-capita leaf litter consumption. This figure shows the mean of 1000 simulations of the interpolation process. Data sources: swisstopo (2010, 2014), Vector25 and TLM3D, DV 5704 000 000, reproduced by permission of swisstopo/JA100119.

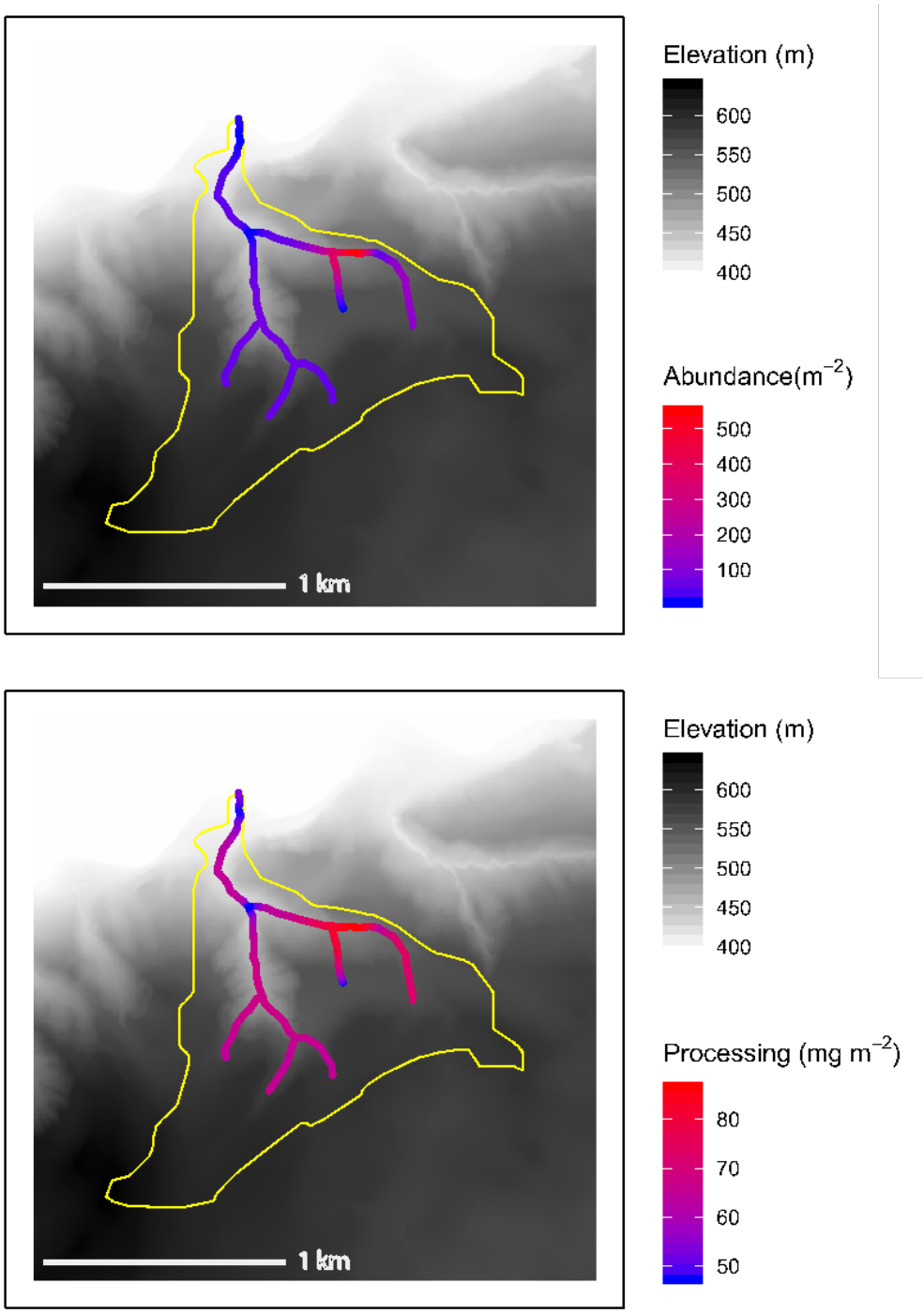

Figure S13. Hotspots of abundance (top panel) and leaf litter processing (bottom panel) in the Unnamed Stream #2 catchment (outlines in yellow), based on upscaling abundance data from 10 sampling points up to longitudinal abundance distributions using inverse distance weighted interpolation. Processing rates (per day) were calculated by multiplying the interpolated abundance in a 1 m section of stream length by the experimentally-derived negative power relating *G. fossarum* density to per-capita leaf litter consumption. This figure shows the mean of 1000 simulations of the interpolation process. Data sources: swisstopo (2010, 2014), Vector25 and TLM3D, DV 5704 000 000, reproduced by permission of swisstopo/JA100119.